KnE Engineering

Conference Paper

Thermal Experiments for Validation of 3-AMADEUS Cubesat

Daniel Carvalhais[1], Paulo Figueiredo[2], Miguel Machado[2], André Guerra[2], and Francisco Brójo[2]

[1]University of Beira Interior
[2]CEiiA

Abstract

There has been an increasing interest in CubeSats missions due to its small size, low cost and flexibility to accommodate different payloads. It enables CubeSats to perform a range of various missions. One of the causes of failure in a satellite in space are the temperature peaks suffered during a full orbital cycle. Therefore, proper thermal control system design and test should be performed to guarantee the reliability of a spacecraft prior to launch.The present work aims to analyze the main heat transfer processes within a satellite to validate the 3-AMADEUS CubeSat and current methodologies used by CEiiA for nano and micro satellites. Hence, with the purpose of developing thermal models with higher reliability, an experiment was devised to be performed in a controlled environment. The experimental test consists in a study of the heat exchange between two aluminum plates through radiation, using infrared lamps as heat source. Three distance configuration and two lamp types are tested. This would emulate the heat transmission between different components within the satellite. The view factors are changed. In parallel, a finite element software (MSC Nastran) is used to carry out a numerical study of the same experiments. The temperature distribution results of both numerical and experimental solutions are then compared, and the results are discussed.

Keywords: Radiation, View factors, Experimental

Corresponding Author:
Daniel Carvalhais
a33876@ubi.pt

🔓 OPEN ACCESS

1. Introduction

Since the first satellite was put in orbit over 50 years ago, satellites have increased in size and weight and consequentially the cost to launch them into space increased as well [1]. However, small satellites more properly, CubeSats have gained a particular interest and are revolutionizing the future of spaceflight. During the orbital cycles the satellite is exposed to intense periods of direct sunlight, or when in eclipse, periods of extreme coldness, resulting in critical temperature peaks which could cause the failure of the full system. Furthermore, the heat produced inside the satellite by electronics must be conducted to the external faces to be rejected through radiation to the surrounding environment. Therefore, a thermal control system is a critical system of satellite. The

global thermal control of a spacecraft is achieved by balancing the heat rejected by the body against all the incident heat loads and the internal heat generated by the electronic subsystems (some of the power used by the electronics is released in the form of heat loads). Thermal radiation as one of the heat transfer mechanisms is extremely important in engineering. Correctly determined radiative heat transfer is a key parameter in the design process of satellites. One of the main goals of the aerospace industry is the development of designing tools and methods for accurate thermal analysis of spacecraft. In general, thermal analysis are performed using a finite element method implemented by a computer software. These programs transform the spacecraft into a mesh and compute the heat transfer between nodes. The boundary conditions are given by the external heat loads and the heat is conducted through the mesh. Ultimately it is possible to know the temperature in each node and therefore heat fluxes. In order to be confident that the spacecraft can handle the vacuum and temperature range without being damaged, thermal verification tests must be performed. The main objectives of thermal testing are: looking out for environmental stress, turn-on capabilities and survival demonstration [2]. The tests can be divided in two categories. One that confirms the validity of thermal control and other that endorse component's integrity and workmanship [3].

2. Methods

All bodies emit and absorb electromagnetic energy when their temperature is above absolute zero. This process is known as thermal radiation, which is ruled by the amount of radiant energy emitted by a blackbody per unit time and per unit area Eb, also known as Stefan-Boltzman law, which states that total energy emitted is proportional to absolute temperature to the fourth power. Greybody surface-to-surface thermal radiation is given by Stefan-Boltzmann's equation, which defines the net heat exchange between two surfaces as:

$$q_{1 \leftrightarrow 2} = \sigma(\epsilon_1 T_1^4 - \alpha_2 T_2^4) A_1 F_{1-2} = \sigma(\epsilon_1 T_1^4 - \alpha_2 T_2^4) A_2 F_{2-1} \tag{1}$$

where e is surface emissivity, s is the Stefan-Boltzmann constant, T is the absolute temperature of the greybody and A is the surface area. F1·2 is the view factor which is defined as as the fraction of radiation leaving surface m that strikes surface n [4]. The view factors only depend on the geometry, size, orientation and distance between the surfaces. Considering two differential areas as shown in Figure 1 it's possible to determine the differential view factor between them by:

$$F_{dA_1 \to dA_2} = 1 A_1 \int_{A_2} \int_{A_1} \cos\theta_1 \cos\theta_2 \pi r^2 dA_1 dA_2 \tag{2}$$

View factors can be calculated using analysis, numerical methods and analogy. The calculation presented is not practical, because even for simple geometries the integrations can be very difficult and complex. For the purpose of this study and for common geometries, such as that found in CubeSats, view factors are given in analytical, graphical and tabular form in several publications [5]. MCS Nastran has two independent routines available for the calculation of view factos between gray diffuse surface elements. The default routine, the VIEW module, relies on a user defined combination of area and contour discretization to determine the geometric view factors. The second module, VIEW3D, utilizes Gaussian integration and semi- analytic contour integration to evaluate view factors [6].
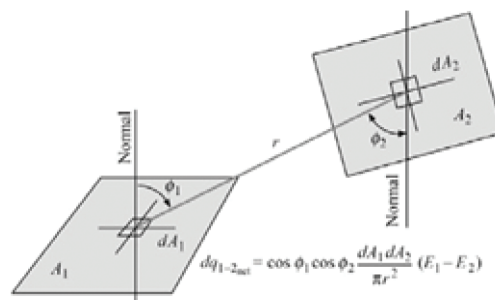
Figure 1: Radiative exchange between two area elements [4].
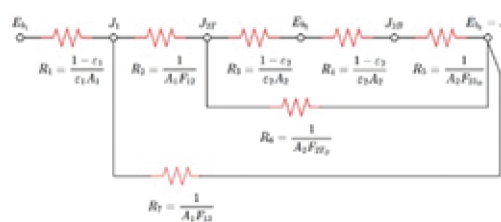
Figure 2: Radiation network for two plates exchanging heat between them and the ambient.

3. Experimental Study

In the experiment it was intended to obtain the heat transfer through radiation between two square aluminum plates (100x100mm). In different setups, the plates can be separated by 20, 50 and 100mm. During the experiments one of the faces is heated by an infrared lamp connected to a regulated power supply. The lamp is positioned outside the vacuum chamber at a fixed distance and concentric with the plates. The other faces of the plates exchange heat between them and with the surrounding environment. Furthermore, it is possible to run the test with the plates hinged at 90° degrees although

it was not done. With these different configurations the view factors are expected to change, thus changing the heat fluxes and plate temperatures.
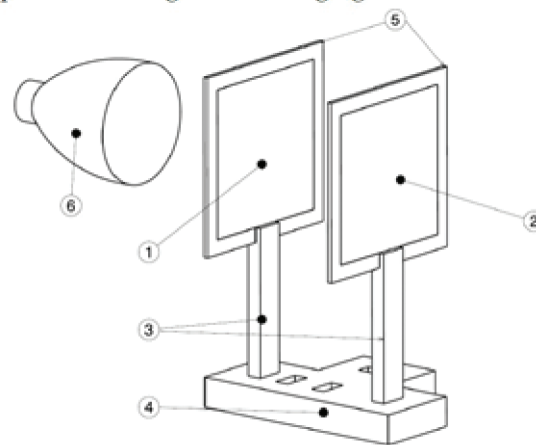
Figure 3: Experimental test rig.

TABLE 1: Label of Figure 3.

1 →	Plate 1
2 →	Plate 2
3 →	Vertical supports
4 →	Main support
5 →	Side cork insulator
6 →	Heating element

The experimental test rig (Figure 3), consists of a wood main support which holds vertical supports which in turn hold both emitter and receiver plates. The main support has several holes that allow to place the plates at different distances. In order to simulate adiabatic conditions, all sides of the aluminum plates are insulated with cork. Apart from that, it is assumed that there is no heat transfer by conduction from the plates to the vertical wood supports due to the low conductivity of wood. Each plate was monitored with at least two thermocouples positioned at the middle and the corner.

Besides the different distance between plates two types of lamps were tested. One was a ceramic infrared bulb with 100 W and a diameter of 75mm. This lamp did not emit any light thus having very high efficiency converting power into heat. Furthermore, the heat was distributed uniformly across the flat lamp face. The second lamp is a common incandescent infrared heat lamp with 150 W and 125mm, which emitted a red light. Both lamps were powered by a ceramic socket in a desk lamp support which allowed to adjust the position of the lamp relatively to the experiment.

In Figures 4(a) and 4(b) it is possible to identify the experimental rig positioned inside the chamber with both lamp configurations. Since the lamps were outside the chamber,

it was constructed a funnel in cardboard to avoid dispersion of heat. It also prevented unintentional heating of the second plate. The first lamp was inside this funnel and thus more protected from cooling by convection. The second lamp was only leaning against the funnel more prone to convection cooling.

(a) 100W Ceramic bulb   (b) 150W Incandescent bulb
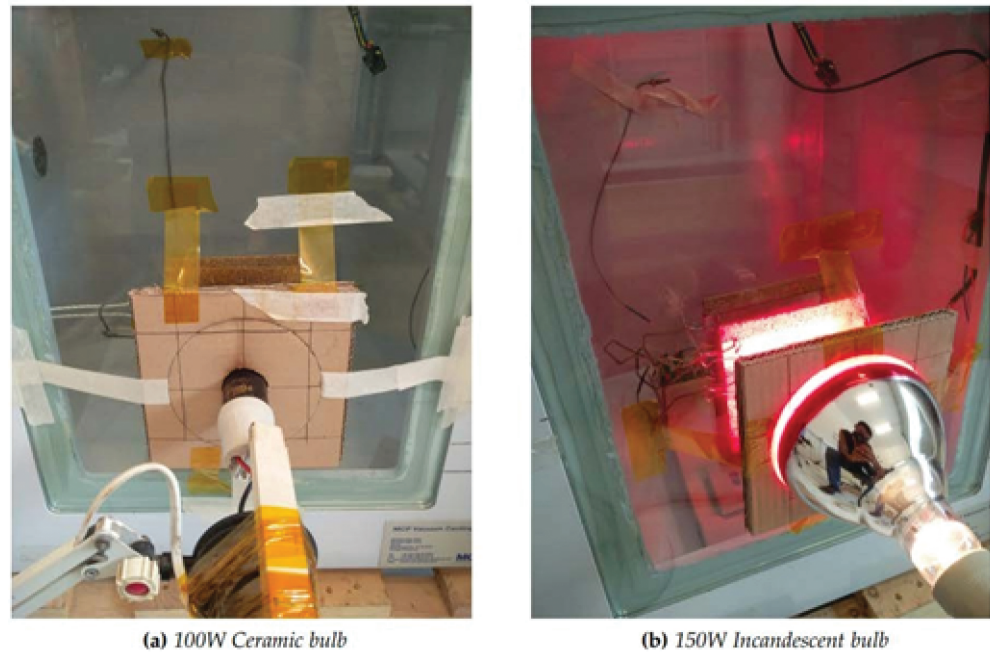
Figure 4: Experimental test rig inside the vacuum chamber.

The emissivity of aluminum plates is an unknown parameter with high influence in thermal analysis. Thus, it was performed a small experiment to estimate it and reduce the error associated with the use of a tabulated value. In the first place the temperature is measured with thermocouples. Afterwards, the emissivity value in thermal camera FLUKE TiS45 is adjusted accordingly, until it matches the temperature previously measured with the sensor. It was estimated an emissivity of 0.4 for the aluminum plates used in five different measures. The data acquisition system used in these experiments was composed of six thermocouples and respective amplifiers, two Arduinos UNO and XBEE modules. One Arduino was inside the vacuum chamber powered by a 5V battery and sending the gathered data via a XBEE wireless link. Connected to the computer was a second Arduino which received the data, exported and stored it in excel in real time for subsequent analysis. Thermocouples were calibrated with two water points as suggested in literature.

4. Numerical Analysis

Considering it was impossible to quantify the heat flux incident upon the first plate, the method proposed consisted in establishing the first plate and ambient temperatures, as obtained in the experimental tests. With this approach the temperature of the second plate is the variable unknown and seek. This analysis can be illustrated by a radiation network method (Figure 2 which represents the physical situation). To build it a "surface resistance", (1 − e)/eA, is connected to each surface and a "space resistance",1/AiFij, between radiosity potentials. This type of analysis is very similar to the methods of analysis used in dc circuit theory, applying also the Kirchoff's current law.

The methodology used for the numerical analysis was the following: Firstly both plates are designed, meshed, properties and temperature constraints are given in HyperMesh. Afterwards, the input file is run in MSC Nastran. Finally, the output file with results are viewed and analyzed in HyperView.

5. Experimental Results

After all the considerations presented previously, the experimental tests were performed. Since each test was repeated at least three times, the results presented are average values with the respective standard deviations. Tables 2 present the measurements for two different heating element configurations. The first plate is the closest to the heating element, thus receiving all the incoming flux. The second plate is the one that is behind only being heated by he first plate. Represented by the D is the distance between plates. Additionally during all tests the ambient temperature inside the chamber was monitored. Each table is followed by a respective graph (Figure 5), to better visualize and analyze the gathered data.

TABLE 2: Results obtained during experimental tests (Ceramic and Incandescent Bulb, respectively).

D [mm]	Temperatures [°C]			D [mm]	Temperatures [°C]		
	First Plate	Second Plate	Ambient		First Plate	Second Plate	Ambient
20	114.5 ± 0.43	64.25 ± 0.22	29.75 ± 0.87	20	163.42 ± 4.40	74.20 ± 4.13	30.00 ± 1.00
50	100.44 ± 2.86	41.63 ± 0.46	29.75 ± 0.87	50	157.06 ± 5.07	49.94 ± 2.73	29.13 ± 0.78
100	99.19 ± 0.63	37.69 ± 1.03	30.38 ± 1.01	100	149.58 ± 7.84	37.79 ± 1.91	29.67 ± 0.72

As can been observed, both tests show the same trend in all measurements. The plates temperatures decrease whenever the distance between them increase. As the distance increases the view factors between the plates decrease from 0.7 up to just 0.2. In other words, a substantial amount of energy does not reach the second plate.

(a) 100W Ceramic bulb

(b) 150W Incandescent bulb
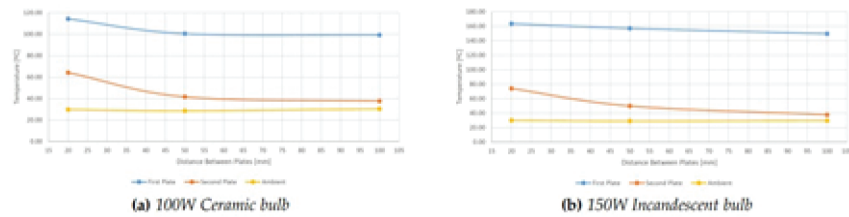
Figure 5: Plotted experimental data.

Furthermore, when the distance is 20mm it is verified that temperatures are higher than the other two cases, 50mm and 100mm. From 50mm up to 100mm it is possible to identify a value convergence which means and goes with the predicted behavior.

As expected, the higher temperatures were achieved with the Incandescent Lamp which has more power that the Ceramic Bulb, 150W vs 100W. Another observation worth mentioning, is the fact that the ceramic bulb took a longer time to reach a steady state temperature than the Incandescent one. As mentioned previously, alongside the temperatures, the respective standard deviations between runs are presented. It is found that the Incandescent Bulb case presents higher deviations between measurements than the first case. This occurrence can be justified with the fact that the lamp was more prone to convection interference than the ceramic one. Thus, a higher experimental error being associated to the last experiment. Add to the previous said during the tests the door room was opened and closed several times. Throughout the day and consecutive days, the ambient temperature outside the chamber fluctuated out of control (cooler temperatures during the morning and hotter temperatures during the afternoon). Finally, it was observed that a large area of the glass chamber door surrounding the funnel was hot, suggesting that a quantity of heating flux was being absorbed by the glass and latter re-emitted to the inside and outside the chamber, heating the second plate

6. Numerical Results

It was observed that both analytical and numerical methods produced the same temperature results. The first plate and ambient temperatures were fixed by the mean measurement given by the experimental data. Figures 6 show plotted temperature values for the second plate and the difference between them. Table 3 shows the temperature of the second second plate and the error % between experimental and numerical results.

(a) *100W Ceramic bulb*

(b) *150W Incandescent bulb*
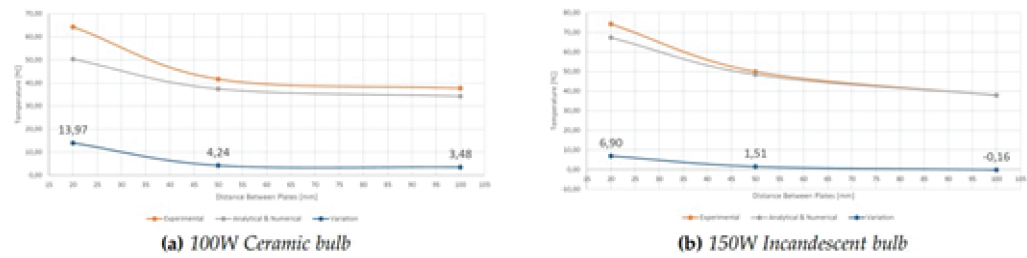
Figure 6: Comparison of results obtained for the second plate between the experimental and numerical for Ceramic and Incandescent Bulb, respectively.

TABLE 3: Error % between experimental and numerical Results (Ceramic and Incandescent Bulb, respectively).

D [mm]	Temperature [°C]		%Error
	Experiment	Numeric	
20	64.25	50.28	21.7
50	41.63	37.39	10.2
100	37.69	34.21	9.2

D [mm]	Temperature [°C]		%Error
	Experiment	Numeric	
20	74.21	67.31	9.3
50	49.94	48.43	3.0
100	37.79	37.95	-0.4

Observing the numerical results is possible to identify a similar trend as it was seen with the experimental results. The second plate temperatures decrease as the distance between plates increases. Comparing the expected temperatures for the second plate with the numerical obtained, it possible to observe a maximum deviation of 14°C for the Ceramic Bulb. In the view of the author, the high errors associated to the distance of 20mm, on both configurations, were associated to the fact that the glass heated in an area greater than the shadow of the first plate. Thus, heating the second plate unintentionally, contributing to the higher temperatures observed. This unwanted heating becomes less relevant as the distance increases.

As for the lower error obtained in the three measurements with the Incandescent bulb the author suggests it may be due to the different methods of heating technology between the lamps. It was verified that as soon as the Incandescent lamp was powered, it was possible to sense incoming flux whereas this was not occurring with the other lamp. Another possible source of error could be the small size of the vacuum chamber, the fact that the walls were painted white and the "low vacuum" achieved by the pump (930mbar). In the numerical analysis the vacuum is considered perfect and the enclosure is assumed as a black body at a constant temperature.

7. Conclusions

Several configurations such as two parallel plates at different distances and two types of heating element were tested and analyzed. Results are presented in this paper. Experimental data for the temperatures of both the emitter and receiver considered

shows a logical trend for both lamp configurations. The temperatures decrease as the distance between plates increases. The difficulties suffered throughout the tests interfered directly in the results observed, showing better results for higher distances between the plates. The higher error observed, 21.7%, was for a 20mm separation between plates and the Ceramic Bulb as a heat source. Above all, the experimental data was satisfactory and within acceptable errors. The tests allowed to realize the capabilities of the actual hardware available for thermal tests. Also, what is needed to turn them more trustworthy in order to perform future reliable thermal analysis of satellites. Above all the current methodologies for thermal radiation analysis were validated.

References

[1] J. P. James Wertz, David Everett, *Space Mission Engineering: The New SMAD (Space Technology Library, Vol. 28).* Microcosm Press, 2011.

[2] D. G. Gilmore, *Spacecraft Thermal Control Handbook, Volume I: Fundamental Technologies.* American Institute of Aeronautics and Astronautics, 2002.

[3] R. Karam, *Satellite Thermal Control for Systems Engineers.* American Institute of Aeronautics and Astronautics, 2012.

[4] J. P. Holman and S. Bhattacharyya, *Heat Transfer, special in ed.* McGraw Hill Education, 2008.

[5] Y. A. Engel, *Heat and Mass Transfer: A Practical Approach.* McGraw-Hill, 2006.

[6] H. P. Lee and J. B. Mason, *"Nastran thermal analyser: A general purpose finite-element heat transfer computer program,"* NASA TMX-2637, 1972.